Biomass Conversion and Biorefinery (2019) 9:421–431
https://doi.org/10.1007/s13399-018-0361-3

ORIGINAL ARTICLE

Production and optimization of NaCl-activated carbon from mango seed using response surface methodology

Aaron Dzigbor[1] · Annie Chimphango[1]

Received: 30 August 2018 / Revised: 1 December 2018 / Accepted: 3 December 2018 / Published online: 3 January 2019

Abstract

Granular activated carbon (AC) produced from mango seed husk through chemical activation with NaCl has potential application in adsorption cooling system. The study investigated the relationship among process parameters and effects on physicochemical and functional properties of AC. Production conditions were optimized using response surface methodology for impregnation ratio (0.25, 0.5, and 0.75), soaking time (2 h, 4 h, and 6 h), and activation temperature (400 °C, 450 °C, and 500 °C). Surface area, ash content, and bulk density were response variables. The AC was produced with comparable quality to commercial AC. Impregnation ratio, soaking time, and carbonization temperature, but not their interaction, had significant effects ($p < 0.05$) on AC surface area, ash content, and bulk density. Optimum production conditions for soaking time, impregnation ratio, and carbonization temperature were 4 h, 0.25, and 500 °C, respectively, which gave BET surface area, ash content, and bulk density of 415 $m^2\ g^{-1}$, 6.92%, and 243 kg m^{-3}, respectively.

Keywords Activated carbon · Chemical activation · Optimization · Response surface methodology

1 Introduction

Mango processing generates a variety of residues including the seed, which consists of a husk and a kernel. The mango seed kernel contains carbohydrates (58–80%), protein (6–13%), and essential amino acids and lipids (6–16%) [1], and it is a good source of phenolics, carotenoids, vitamin C, and dietary fiber that can improve human health and nutrition [1, 2]. As a result, there is a potential for biorefining of the mango seed kernel into such low-volume but high value-added products. The mango seed husk, on the other hand, has less commercial value compared with the mango seed kernel, and it is therefore disposed of into the environment, which causes pollution, or used as compost [1]. One of the ways to add economic value to the mango seed husk is through the production of activated carbon. Therefore, together with biorefining of the mango seed kernel, it can potentially increase the economic value of the mango seed as a feedstock in a biorefinery. Activated carbon is one of the commonly used adsorbents [3] in several applications including removal of dyes, odors, and contaminants, in water purification processes as well as in adsorption cooling processes [4–6]. The functional properties of activated carbon are among the other factors influenced by the production method. Activated carbon can be produced through physical and chemical means. The physical activation method, which is generally applied to non-renewable feedstocks such as coke, pitch, and coal [7], involves carbonization in an inert atmosphere [8–11] followed by activation using steam (800–1000 °C) or carbon dioxide [12]. Such physical activation method is costly due to its high carbonization temperature, high processing time, and low carbon yield [7] and has high safety risks for small-scale applications. Unlike the physical activation method, the chemical activation method which is applied to biomass materials is economically feasible due to its shorter processing time, higher activated carbon yield [7], and lower activation temperature (400–500 °C) [6, 13–15].

Activated carbon from biomass materials such as the mango seed husk is produced through chemical means where carbonization and activation occur simultaneously [8, 11, 12, 16–18]. The activation chemicals are added before reaching the carbonization temperature of 400–500 °C [6, 13–15]. Many chemicals such as $CaCl_2$, $ZnCl_2$, H_3PO_4, K_2CO_3, and KOH have been used for the production of activated carbon

✉ Annie Chimphango
achimpha@sun.ac.za

[1] Department of Process Engineering, Stellenbosch University, Stellenbosch 7600, South Africa

[6, 12, 19, 20]. Each of these chemicals affects pore formation differently and has different safety concerns that affect the application of the activated carbon produced. For example, H_3PO_4 restricts the escape of the tar from the carbon during carbonization, thus affecting the development of pore structures [21]. The KOH, on the other hand, is normally applied to already carbonized materials because of their lower activated carbon yield when virgin biomass is used than other activating chemicals such as H_3PO_4 and $ZnCl_2$ [7]. Similar to $ZnCl_2$, the NaCl is a strong dehydrating agent, which prevents the formation of tars and enhances the release of volatile matters from the carbon and the formation of well-developed pore structure in the carbon [7]. Furthermore, NaCl is not as toxic as other chemicals. The NaCl has a boiling point of 1465 °C, which is higher than the carbonization temperature, and, thus, does not decompose during carbonization to produce hazardous fumes [22, 23]. On the other hand, the H_3PO_4 and $ZnCl_2$ with boiling points of 213 °C and 732 °C, respectively, may decompose at the carbonization temperature to produce toxic fumes [22, 23]. Arguably, KOH has a boiling point of 1327 °C, which is equally higher than the typical carbonization temperatures [7]. However, the presence of KOH in the effluent during the washing stage may be hazardous to the environment and humans [7]. Consequently, activated carbon produced using NaCl activation may be suitable for application in pharmaceutical and food industries unlike that from KOH and $ZnCl_2$ activation due to safety and contamination issues [7]. The time-weighted average recommended an airborne exposure limit for NaCl of 5–10 mg m^{-3} [24] while those of $ZnCl_2$ and H_3PO_4 are 1–2 mg m^{-3} [22, 23].

The NaCl is considered to be an effective catalyst for activated carbon production from wood sources [25]. Besides, NaCl has a high thermal conductivity than most of the chemicals used [26], which can increase the rate of heating the mango seed husk during carbonization, and, thus, becomes superior to other activation chemicals. Furthermore, most of these activation chemicals are not readily available for small-scale production. NaCl can be easily accessed at a small-scale level.

The use of NaCl as an activating agent in the production of activated carbon from non-wood sources has been reported for the production of powdered activated carbon from mango seed husk [27] but not for granular activated carbon. Powdered activated (< 0.045 mm) carbon is normally suited as an adsorbent in wastewater treatment whereas granular activated carbon is suited for applications such as adsorption cooling because of its high diffusion rate through the adsorbent bed and for not being easily sucked out of the adsorber during vacuum creation [28].

The physical and functional properties of activated carbon apart from the type of activation chemical are affected by soaking time, carbonization temperature, and particle size [9, 15]. Therefore, it is important to understand the effects of the impregnation ratio, soaking time, and carbonization temperature on the properties of the activated carbon. This study aimed to investigate the production of granular activated carbon from mango seed, targeting specifically the husk, through NaCl activation, as a potential adsorbent in the adsorption cooling system. The husk is targeted instead of the whole mango seed for the production of the activated carbon in order to allow potential integration with mango seed biorefinery, which would produce low-volume but high value-added bioproducts. Specifically, the study assessed the optimum production conditions for making the granular activated carbon from the mango seed husk by simultaneously considering the effects of NaCl impregnation ratio, soaking time, carbonization temperature, and the interaction of these parameters on the physicochemical and functional properties, including surface area, ash content, and bulk density using response surface methodology (RSM) [29].

2 Materials and methodology

2.1 Materials

The NaCl (99.5% in purity) was purchased from Kimix Chemical and Laboratory Supplies CC. Tommy Atkins mango kernels were kindly donated by Hoedspruit Fruit Processors (South Africa). Nitrogen gas (technical grade; 99.5% purity) 5.0 (Afrox Ltd.) was used for the pyrolysis of the mango husk, while carbon dioxide and liquid nitrogen baseline 5.0 (Afrox Ltd.) were used in the characterization of the activated carbon.

2.2 Mango husk preparation and characterization

Pre-dried Tommy Atkins mango kernels were obtained from Hoedspruit Fruit Processors (South Africa). The mango kernels were opened to separate the seeds from the husk. The mango husks were reduced into sizes ranging from 1 cm to 2 cm using a pair of scissors. The resulting mango husks were dried in an oven at 105 °C for 24 h until a constant weight was reached. A sample of the mango husks was milled in a Condux-Werkbei (Hanau) mill. The resulting particles were then sieved using a Vibratory Shaker Retsch AS200. The fractions that were retained on 425 μm and 625 μm were used for chemical analysis. The samples were subjected to a proximate analysis based on ASTM standards as follows: moisture [30], ash content [31], volatile matter [32], and fixed carbon. The lignocellulosic composition of the material was determined by the NREL method [33].

2.3 Proximate analysis

The fractions (425 μm and 625 μm) were subjected to proximate analysis to determine the moisture, ash, fixed carbon,

and volatile contents, based on the ASTM-E-1131 [30] method using a Metler Toledo TGA/DSC 1 thermogravimetric analyzer. About 24 ± 3 mg of each lignin sample was loaded onto a 600-μl alumina crucible and placed on the TGA pan. Heat was supplied in a sequential manner to remove moisture removal at 110 °C, volatile content removal at 900 °C under nitrogen, and fixed carbon combustion with oxygen at 900 °C.

2.4 Activated carbon production

The procedure for production of the activated carbon from mango husk is shown at Fig. 1. NaCl solutions were prepared to the required impregnation ratios of 0.25, 0.50, and 0.75 defined as the ratio of dry weight of NaCl to the weight of the mango husk based on similar study [27]. Dried mango seed husk sample (100 g) containing sizes ranging from 1 to 2 cm was mixed in a beaker with 250 mL of NaCl solution of specified concentration (10% *w/v*, 20% *w/v*, and 30% *w/v*). The size of the mango seed husk was chosen by taking into account the requirement for producing granular activated carbon, which is suited for application in adsorption cooling systems that involve vacuum creation. Notably, activated carbon produced from smaller sized mango seed would likely be close to powdered form, which could easily be sucked out during vacuum creation. Mango husks were soaked in NaCl solution for a period of 2, 4 and 6 h to obtain impregnation ratios of 0.25, 0.5 and 0.75 at room temperature (25 °C). The impregnated husks samples were dried in an oven at 50 °C for 72 h. The moisture content at the end of the oven drying was about 25%. Approximately 50 g of the impregnated sample was placed in a stainless steel container, which was inserted into the reactor tube of the pyrolysis furnace for carbonization under nitrogen atmosphere, at a flow rate of 1 l min^{-1} and a heating rate of 10 °C min^{-1} (Fig. 2). The carbonization temperatures were 400 °C, 450 °C, and 500 °C, which were chosen based on previous studies. The optimum carbonization temperature for most biomass materials generally falls between 400 °C and 500 °C [4, 9, 15, 34]. Once the carbonization temperature was reached, the samples were kept constant at the carbonization temperature for 1 h. At the end of this process, the flow of the nitrogen gas continued to avoid carbon reacting with oxygen at high temperature to produce CO_2 which could lead to a loss of carbon. After carbonization, the sample was cooled down outside the furnace at room temperature.

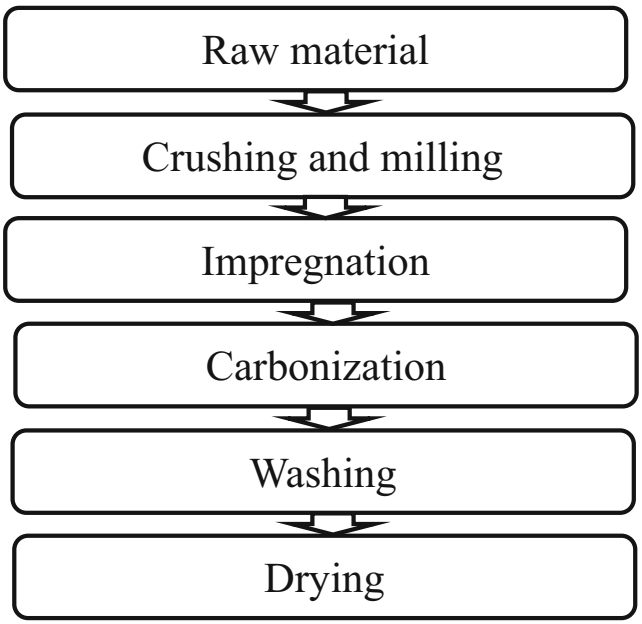

Fig. 1 Process flow for the production of mango seed husk activated carbon using NaCl. The activated carbons produced were rinsed with demineralized water several times to remove any excess NaCl that did not react. The activated carbon was dried in an oven at 105 °C for 24 h to evaporate the water until constant weight was reached. The dried activated carbon was placed in a sealed container and stored in a desiccator

2.5 Experimental design and statistical analysis

The experiments for the production of the activated carbon were carried in a 3^3 Box-Behnken fractional factorial [29] designed experiment with three center runs for impregnation ratio, soaking time, and carbonization temperature to give a total of 15 runs. The Box-Behnken fractional factorial was used because the optimum values were expected to be within the limits set for each variable [15]. The dependent variables (responses) analyzed are yield, bulk density, ash content, and surface area. Commercial activated carbon was used as the benchmark in this study.

2.6 Activated carbon characterization

The yield of activated carbon produced was determined using the relation shown in Eq. (1):

$$\text{Yield}\ (\%) = \frac{W_1}{W_0} \times 100 \tag{1}$$

where W_1 is the dry weight of the final activated carbon and W_0 is the dry weight of the precursor material. The bulk density was determined by a standard method [34–36]. Samples of activated carbon were weighed into a known volume graduated cylinder and tapped gently until the volume of activated carbon remained constant in the cylinder. The bulk density was calculated as the ratio of the weight of the activated carbon to the known volume of the closely packed sample. Ash content was determined by a standard method [35]. Since chemical activation normally produces narrow pores [11, 37, 38] and nitrogen has a problem of diffusion of the molecules inside the narrow pores (< 0.7 nm) [39], it was suggested to use CO_2 for characterization of micropores to complement to

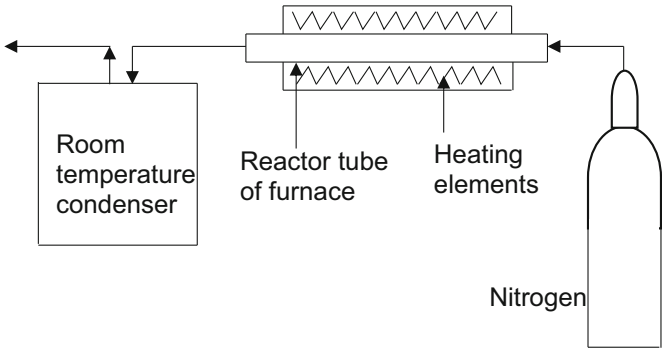

Fig. 2 Setup for pyrolysis of the treated mango husk for production of activated carbon

N_2 characterization [38]. Therefore, CO_2 was used for the characterization of the activated carbon to be used in the optimization process. After that, N_2 characterization was performed on the optimized product. The CO_2 characterization of the activated carbon was done using a 3Flex surface characterization instrument from Micromeritics Instrument Corporation (Micromeritics ASAP 2020). About 0.3–0.6 g of each activated carbon sample was first freed of moisture and atmospheric vapor by application of electrically induced heat and evacuation in a VacPrep 061 degasser (Micromeritics Instrument Corporation). The sample was heated to 90 °C with a vacuum pump run and held for 1 h and thereafter heated to 250 °C and kept at this temperature for 20 h while the vacuum was still running. Thereafter, the sample was transferred to the 3Flex instrument (Accelerated Surface Area and Porosimetry System, Micromeritics Instrument Corporation) where in situ degassing was done at a temperature of 175 °C with a vacuum pump run for 1 h. The sample temperature was then reduced to that of CO_2 (273 K) at a relative pressure range (P/P_0) of 0.00005–0.025. The CO_2 gas was then admitted in an incremental dosage of 3.0 $cm^3\ g^{-1}$. Surface area and pore volume were determined on CO_2 adsorption isotherms measured at 273 K, and the accumulated gas quantity adsorbed and CO_2 gas pressure data at that temperature (273 K) were then graphed to generate an adsorption isotherm. The isotherm data were then treated in accordance with BET theory [40] to arrive at a specific surface area. These results were used for the optimization process through desirability analysis. The characterization of the activated carbon was done using N_2 by following similar steps. However, in this case, the sample temperature was then reduced to that of liquid nitrogen (77 K) after degassing. Nitrogen gas was then admitted in an incremental dosage of 3.0 $cm^3\ g^{-1}$. Surface area and pore volume were determined on N_2 adsorption isotherms measured at 77 K at a relative pressure range (P/P_0) of 0.0000002–0.1026. The accumulated gas quantity adsorbed and N_2 gas pressure data at that temperature (77 K) were then graphed to generate an adsorption isotherm. The isotherm data were then treated in accordance with BET theory [40] to arrive at a specific surface area.

2.7 Regression analysis and optimization

Regression analysis was performed on data in order to derive appropriate equation for each response. All variable parameters and their interactions were considered for a model for each response. Statistical analysis software (Statistica 13) was used to solve the coefficients of the second-order model with three variables for each response as shown below:

$$Y = \beta_0 + \beta_1 X_1 + \beta_2 X_2 + \beta_3 X_3 + \beta_{11} {X_1}^2 + \beta_{22} {X_2}^2 + \beta_{33} {X_3}^2 + \beta_{12} X_1 X_2 + \beta_{13} X_1 X_3 + \beta_{23} X_2 X_3 \quad (2)$$

where β_0, β_1, β_2, β_3, β_{11}, β_{22}, β_{33}, β_{12}, β_{13}, and β_{23} are the regression coefficients; X_1, X_2, and X_3 are the coded independent variables/regressors for soaking time, impregnation ratio, and carbonization temperature; and Y is the particular response evaluated. Predicted values were solved from the derived equations for each of the response. The relationship of each response variable to the input variable was evaluated for its significance at a probability value of lower than 0.05 ($p < 0.05$), and the strength of the relationship was evaluated using regression coefficient (R^2). Subsequently, a lack-of-fit test was performed to show the adequacy of the model at $p > 0.05$. In addition, normal distributions of the residuals were checked to validate the assumptions made in the ANOVA [29]. Identification of the optimal production conditions involved surface plots (contour plots) of the effect on two variables while holding one at a set target. In addition, the desirability function approach has been used to obtain the production conditions at which the responses exhibit the ideal optimal value (maximum).

2.8 Fourier transform infrared spectroscopy analysis of surface functional groups on the activated carbon

The changes in surface functional groups on the activated carbon were surface analyzed using Fourier transform infrared spectroscopy (FTIR) in a Thermo Scientific Nicolet iS10 apparatus equipped with smart ITR diamond attenuated total reflectance (ATR). The experiments were carried out in the

wavelength range of 250 cm^{-1} to 4500 cm^{-1} with the resolution of 4 cm^{-1} and total scans of 64 for each sample. This analysis was done to analyze the changes in the functional groups of the raw mango seed husk at different carbonization temperatures.

3 Results and discussion

3.1 Mango seed husk characterization

Characterizations of feedstock are important for determining the functional properties and quality of the activated carbon that can be formed [13, 41]. The chemical composition analysis (Table 1) indicates that the mango husk contains about 4.24% moisture, 19.56% fixed carbon, 74.43% volatile matter, and 2.73% ash (Table 1).

The percentage of lignin, hemicellulose, and cellulose is comparable to what is reported in the literature of 5–20.71%, 15.6–16.63%, and 34.68–39.4%, respectively [42, 43]. Furthermore, the higher the content of volatile matter, the greater the porosity and, subsequently, the higher the surface area of the activated carbon produced [11]. According to Suhas and Ribeiro Carrott [13], materials with a greater content of lignin produce activated carbon with a predominantly macroporous structure, while raw materials with a higher content of cellulose produce activated carbon with a predominantly microporous structure.

3.2 Effect of production conditions on characteristics of the activated carbon

Varying the impregnation ratio, soaking time, and carbonization temperature resulted in the production of activated carbon with different characteristics in terms of surface area, ash content, and bulk density (Table 2). High carbonization temperature provided activated carbon with high surface area, low ash content, and bulk density (Table 2). The contour plots (Fig. 3a–c) show the trends for the effects of each parameter and interactions of the parameters on the specified responses for the activated carbon. The surface area of the activated carbon increased with increased soaking time and carbonization temperature (Fig. 3a (i and iii)). The surface area is a measure of the porosity of activated carbons on which adsorption can take place. The relationship between the surface area and the impregnation ratio was different from that of carbonization temperature. The surface area decreased with an impregnation ratio up to a value of 0.45, and thereafter, the surface area increased (Fig. 3a (ii and iii)).

Thus, the greater the impregnation ratio (beyond 0.45), coupled with either longer soaking times or high carbonization temperature, the higher the surface area for adsorption (Fig. 3a (i–iii)). The impregnation ratio and carbonization temperature were the two parameters that showed significant effects ($p < 0.05$) on the surface area (Fig. 4a). However, the carbonization temperature had the greatest positive impact on the surface area of the activated carbon, whereas the impregnation ratio had the most negative effect (Fig. 4a). The increase in carbonization temperature increased the surface area (Fig. 3a (i and ii), which can be attributed to the degradation of the hemicellulose, cellulose, and lignin that produces volatile compounds, bio-oil, and carbon [13]. The degradation of these compounds, similar to dissolution by NaCl, leads to further opening of pores in the seed husk structure. However, the degradation of these components does not occur at the same temperature [44]. For example, thermal degradation of hemicellulose, cellulose, and lignin would occur between 220 °C and 315 °C, between 315 °C and 400 °C, and between

Table 1 Proximate analysis and lignocellulosic composition of mango seed husk

Proximate analysis (wet basis)	Composition (%)
Moisture	4.24 ± 0.04
Fixed carbon	19.56 ± 0.07
Volatile matter	73.43 ± 0.34
Ashes	2.73 ± 0.50
Lignocellulose analysis	
Cellulose	37.28 ± 2.58
Hemicellulose	19.03 ± 1.11
Lignin	23.92 ± 0.05

Table 2 Characteristics of activated carbon produced using the pyrolysis method at different process conditions

Soaking time (h)	Impregnation ratio	Temperature (°C)	Bulk density (kg m^{-3})	Ash content (%)	Surface area (m^2 g^{-1})
6	0.75	450	242	9.59	223
4	0.50	450	212	8.20	173
4	0.50	450	207	6.47	160
4	0.75	400	257	11.70	177
4	0.75	500	192	9.23	215
2	0.75	450	252	10.07	195
4	0.25	500	232	5.94	205
6	0.50	500	203	7.78	215
2	0.25	450	269	5.93	158
4	0.25	400	251	6.00	155
4	0.50	450	238	7.57	202
6	0.50	400	242	8.93	125
6	0.25	450	262	7.52	201
2	0.50	400	272	8.87	116
2	0.50	500	208	6.38	172

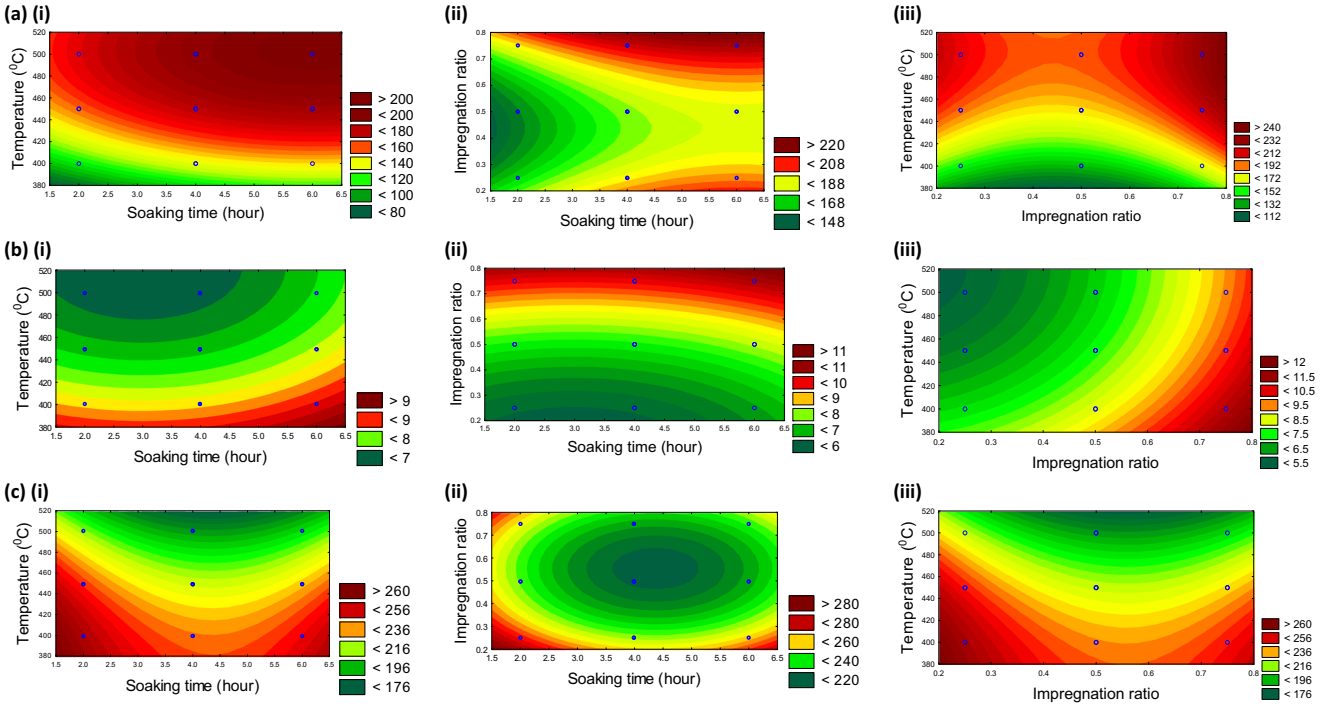

Fig. 3 **a** Effects on the surface area of (i) temperature vs soaking time at 0.50 impregnation ratio, (ii) impregnation ratio vs soaking time at 450 °C, and (iii) temperature vs impregnation ratio at a 4-h soaking time. **b** Effects on the ash content of (i) temperature vs soaking time at 0.50 impregnation ratio, (ii) impregnation ratio vs soaking time at 450 °C, and (iii) temperature vs impregnation ratio at a 4-h soaking time. **c** Effects on the bulk density of (i) temperature vs soaking time at 0.50 impregnation ratio, (ii) impregnation ratio vs soaking time at 450 °C, and (iii) temperature vs impregnation ratio at a 4-h soaking time

160 °C and 900 °C, respectively [44]. Therefore, the higher carbonization temperature of 400–500 °C applied (Table 2) most likely degraded hemicelluloses as well as the cellulose and lignin. The results are similar to the study of Adinata et al. [14] where activated carbon produced with both KOH and K_2CO_3 as activation agents showed similar trends for such temperature ranges.

The increase in soaking time increased the surface area of the activated carbon alone and also in interaction with impregnation ratio and carbonization temperature. The effect suggests that during manufacturing of activated carbon, these parameters may have to be monitored and controlled simultaneously for optimal surface area. However, since only the temperature (linear) and the impregnation ratio (quadratic) showed significant effects ($p < 0.05$) on the surface area (Fig. 4a), the desired surface area for the activated carbon can be tailored made by controlling the two parameters independently.

The presence of ash in the activated carbon indicates the presence of inorganic content, which reduces its quality [45]. Similar to the surface area, the carbonization temperature and impregnation ratio were the most important factors to consider when high-quality activated carbon is desirable from the mango seed husks. The results show that the effects of these two parameters were significant at $p < 0.05$ on the ash content (Fig. 3b (i–iii)). On the other hand, a combination of high impregnation ratio and longer soaking time is not desirable for high-quality activated carbon because of increased ash content (Fig. 3b (ii)) unless it is accompanied by high carbonization temperature above 450 °C. At the stated temperature, the ash content is less than 8% for soaking times and impregnation ratio of less than 6 h and 0.6, respectively (Fig. 3b (i and iii)). The effect of carbonization temperature on ash content could be because the sodium absorbed in the husk is reduced to metallic sodium at elevated temperatures and is subsequently lost during the washing stage [11]. Similar to the surface area, the impregnation ratio (linear) has the most negative effect on the quality of the activated carbon because of its positive relationship with the ash content (Fig. 4b) whereas the temperature has a negative relationship with the ash content.

Bulk density is an important parameter mainly for handling of the activated carbon in the adsorption cooling system, in particular the adsorbent unit. The bulk density affects the volume that can be handled in the adsorbent unit per unit time.

The bulk density was largely affected by all the three parameters: carbonization temperature, soaking time, and impregnation ratio (Fig. 3c (i–iii)). The effects of carbonization temperature (linear), impregnation ratio (quadratic), and soaking time (quadratic) on the bulk density were significant ($p < 0.05$) (Fig. 4c). Activated carbon of low bulk density from the seed husks can be obtained if the production is done

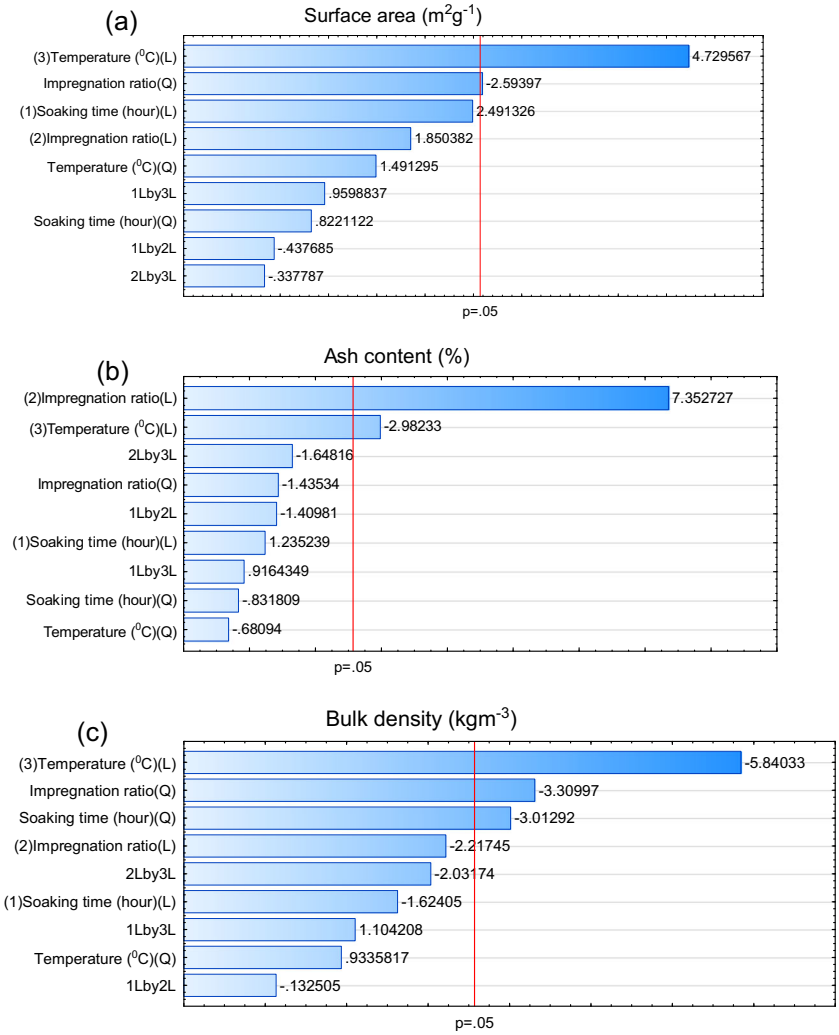

Fig. 4 **a**–**c** Pareto charts showing the size and significance of the effects of activation, temperature, soaking time, and activation temperature on the properties of mango seed husk activated carbon produced using NaCl as an activation agent

using impregnation ratios between 0.5 and 0.6 at temperatures above 500 °C and soaking times between 3.5 and 5.5 h (Fig. 3c (i and iii)). The increase in bulk density at reduced carbonization temperature may be related to the limited breakdown of the structural components (hemicellulose, cellulose, and lignin) [44], which leads to reduced porosity.

3.3 Optimal conditions for the production of activated carbon from mango seed husk

The non-linear regression coefficients for the model (Eq. (2)) are shown in Table 3 (a). The positive relationship between carbonization temperature and surface area is reflected by the positive coefficient whereas the negative relationship with bulk density is reflected by the negative regression coefficient (Table 3 (a)). The experimental data fitted the model for all the three outputs (surface area, ash content, and bulk density) with an adjusted R^2 value of at least 0.8 (Table 3 (b)). The p value from the lack-of-fit test showed that the data fitted the model at $p > 0.05$ (Table 3b). The optimum production conditions were identified to be 5.8 h for the soaking time, 0.25 for the impregnation ratio, and 500 °C for the carbonization temperature (Table 4). The optimum carbonization temperature is comparable to the optimum temperature of 456 °C obtained when $ZnCl_2$ was used as an activating chemical with the optimum impregnation ratio of 1.08, to produce activated carbon from agave bagasse [9].

At the optimized conditions, the mango seed husk activated carbon had a BET surface area of 415 $m^2\ g^{-1}$, an ash content of 6.92%, and a bulk density of 243 kg m^{-3} (Table 4). The BET surface area falls within the range of 3 $m^2\ g^{-1}$ to 1718 $m^2\ g^{-1}$ reported for activated carbon produced from agricultural residues [6]. However, it is lower than the surface area of 618–661 $m^2\ g^{-1}$ for mango seed husk, which used NaCl as an activation agent mainly because the activated carbon produced was in powder form whereas, in this study, it was in granular form [27].

Similarly, activated carbon powder from coal, wood, and coconut was reported to have a higher surface area of 750–850 $m^2\ g^{-1}$, 900–1200 $m^2\ g^{-1}$, and 590–1500 $m^2\ g^{-1}$,

Table 3 Final regression coefficients, after discarding the insignificant terms and values of the statistical test parameters that validate the model

	Surface area (m^2 g^{-1})	Ash content (%)	Bulk density (kg m^{-3})
a. Final regression coefficients, after discarding the insignificant terms			
β_0	173.69	7.74	219.00
β_1	15.37	0.32	− 6.50
β_2	11.37	1.90	− 8.88
β_3	29.25	− 0.77	− 23.38
β_{11}	–	–	17.75
β_{22}	24.04	0.50	19.50
β_{33}	− 13.21	–	− 5.50
β_{12}	–	− 0.52	–
β_{13}	8.50	–	6.25
β_{23}	–	− 0.60	− 11.50
b. Values of the statistical test parameters that validate the model			
Lack-of-fit test	0.8883	0.7998	0.9808
R^2	0.8797	0.9113	0.9309
R^2 adjusted	0.7894	0.8447	0.8387

respectively [46] than the activated carbon from the mango seed husk produced in this study. The activated carbon for the commercial activated carbon had a particle size of 3 mm compared to 10 mm for this study.

The ash content and bulk density of the mango seed husk activated carbon produced in this study were 6.92% and 243 kg m^{-3}, respectively, which shows improved quality when compared with the ash content of 13.55–14.75% for the activated carbon produced by Mise and Patil [27], but it is close to about 6% reported for commercial activated carbon [46]. The bulk density of the mango seed husk activated carbon produced is higher than the 204–232 kg m^{-3} bulk density reported by Mise and Patil [27]. The relatively high bulk density of the activated carbon produced in this study makes it a better choice for use in vapor-phase applications such as adsorption cooling, since it would not be easily sucked out during the vacuum creation process.

3.4 Validation of model production conditions for mango husk activated carbon

Using the predicted optimum production conditions in Table 4 to produce activated carbon, the surface area, ash content, and bulk density of the activated carbon produced were measured to validate the model (Table 5).

The results (Table 5) showed that the values for the surface area (BET_{CO_2}), ash content, and bulk density of the activated carbon produced at the optimal conditions were very close to the predicted values deviating by 2.69%, 1.01%, and 2.06%, respectively. Furthermore, the surface area (BET_{N_2}) obtained when nitrogen gas was used to estimate the BET surface area of the activated carbon produced was found to be 415 m^2 g^{-1} (Table 4), which falls within the surface area of 300–2500 m^2 g^{-1} reported by Campbell et al. [47] for activated carbon.

Table 4 Optimized conditions and predicted values of responses

Parameters	Predicted value	Responses	Optimum value
Soaking time	5.8 h	Surface area[a]	
		BET_{CO_2}	223 m^2 g^{-1}
Impregnation ratio	0.25	Ash content	6.92%
Temperature	500 °C	Bulk density	243 kg m^{-3}

[a] BET_{N_2} = 415 m^2 g^{-1}

3.5 Changes in surface functional groups on the activated carbon as determined by FTIR analysis

The infrared spectral bands (Fig. 5) depicted the changing structure of the various samples of mango seed husk activated carbon. The infrared spectrum of the raw mango seed husk shows the presence of several functional groups such as alkene, aromatic, ketone, hydroxyl, and carboxyl functional groups (Fig. 5). These kinds of functional groups are typical of many lignocellulose raw materials.

Table 5 Validated model production conditions for mango husk activated carbon

Response	Optimized model value	Experimental value	Percentage error
Surface area, m^2 g^{-1} (BET_{CO_2})	223	229	2.69
Ash content, %	6.92	6.99	1.01
Bulk density, kg m^{-3}	243	248	2.06

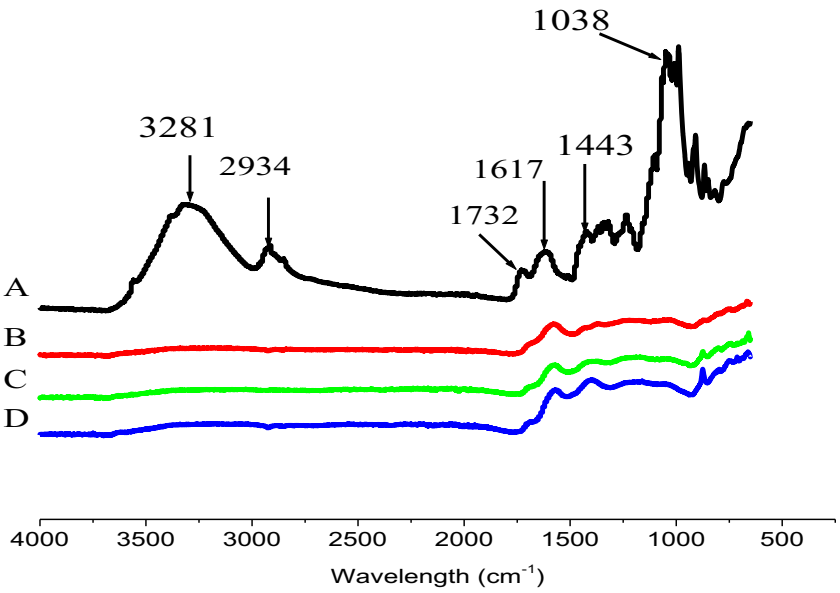

Fig. 5 Comparison of the FTIR spectra of raw mango seed husk (A), mango seed husk activated carbon produced at 500 °C (B), mango seed husk activated carbon produced at 450 °C (C), and mango seed husk activated carbon produced at 400 °C (D)

The absorbance for the hydroxyl stretching vibrations of the water in the raw mango seed husk is correlated to the band at 3281 cm^{-1} [11, 48, 49]. The other bands detected in the raw mango seed husk are C=C (alkene functional group) at 1617 cm^{-1}, C=O (carbonyl functional group) with a spectral band at 1732 cm^{-1}, organic acid (carboxyl functional group) at 2934 cm^{-1}, aromatic group (benzene) at 1443 cm^{-1}, and C–O (ether functional group) at 1038 cm^{-1} [11, 50]. Several of the spectral bands in the raw mango seed husk disappeared with increasing carbonization temperature due to thermal degradation of bonds of the lignocellulosic compounds present. The activated carbon produced at 400 °C and 450 °C showed a small peak at 1617 cm^{-1}, suggesting that there could be cellulose and lignin present. However, the activated carbon produced at 500 °C showed less remnants of lignin because the lignin is totally broken down at such high temperatures [44]. The result supports the optimum carbonization temperature obtained (500 °C) as evident from the absent or reduced absorbance from volatiles initially present in the sample.

Therefore, activated carbon was produced from mango seed husk through simultaneous carbonization and activation with NaCl as the activation agent, which falls within the quality range (in terms of BET surface area and ash content) of commercial activated carbon. There are some precautions to be considered when using NaCl. Although it is a relatively safer activation agent than most activating chemicals, NaCl has some challenges because of the corrosive effect to most metals; therefore, anti-corrosive materials should be used to protect the equipment used for soaking the biomass material and for the adsorber construction. Secondly, the discharged NaCl water needs special disposal procedures to avoid damage to the environment.

4 Conclusion

The optimum mango husk activated carbon production conditions determined using the response surface methodology for impregnation ratio, soaking time, and carbonization temperature were 0.25, 5.8 h, and 500 °C, respectively, which resulted in activated carbon with an ash content of 6.92%, a bulk density of 243 kg m^{-3}, and a surface area (BET_{CO_2}) of 223 m^2 g^{-1}, which was 415 m^2 g^{-1} (BET_{N_2}). These optimal activated carbon production conditions were within the surface area ranges of 300–2500 m^2 g^{-1} found in the literature for similar materials [47]. At the validated production conditions, the ash content (6.69%), the bulk density (248 kg m^{-3}), and the surface area (229 m^2 g^{-1} (BET_{CO_2})) were within 2% error (1.01%, 2.06%, and 2.6%, respectively) of the predicted values, which suggests the possibility of using the model to predict and control the activated carbon production process. Furthermore, the lack of interaction among the production conditions suggests that the production of the activated carbon from mango seed husks can be controlled by varying each parameter independently to tailor make the quality of the activated carbon in terms of surface area, bulk density, and ash content for different applications. Notably, the NaCl is a relatively safe and, potentially, an environment-friendly alternative activation agent for the production of granular activated carbon from mango seed husk of comparable quality to commercial activated carbon as well as to activated carbon from biomass sources. Therefore, the study has provided an optimized process that is not only effective in producing functional activated carbon but has also a potential to reduce the environmental impact of activated carbon production and, at the same time, provide an opportunity for the development of an integrated biorefinery.

Acknowledgements The authors are indebted to Prof. Görgens for providing access to the pyrolysis equipment and the staff at the Analytical Laboratory at Department of Process Engineering, Stellenbosch University, for the technical support in the analysis of samples. The authors are also thankful to Hoedspruit Fruit Processors (South Africa) for providing the mango seeds.

Funding information The authors are grateful for the financial support from the National Research Foundation (NRF) of South Africa under the Research and Technology Fund (RTF) and the Department of Process Engineering, Stellenbosch University.

References

1. Torres-Leon C, Rojas R, Contreras-Esquivel JC, Serna-Cock L, Belmares-Cerda RE, Aguilar CN (2016) Mango seed: functional and nutritional properties. Trends Food Sci Technol 55:109–117. https://doi.org/10.1016/j.tifs.2016.06.009
2. Jahurul MHA, Zaidul ISM, Ghafoor K, Al-Juhaimi FY, Nyam KL, Norulaini NAN et al (2015) Mango (Mangifera indica L.) by-products and their valuable components: a review. Food Chem 183:173–180. https://doi.org/10.1016/j.foodchem.2015.03.046
3. Chakraborty S, De S, DasGupta S, Basu JK (2005) Adsorption study for the removal of a basic dye: experimental and modeling. Chemosphere 58:1079–1086. https://doi.org/10.1016/j.chemosphere.2004.09.066
4. Yakout SM, Sharaf El-Deen G (2016) Characterization of activated carbon prepared by phosphoric acid activation of olive stones. Arab J Chem 9:S1155–S1162. https://doi.org/10.1016/j.arabjc.2011.12.002
5. Matos M, Barreiro MF, Gandini A (2010) Olive stone as a renewable source of biopolyols. Ind Crop Prod 32:7–12. https://doi.org/10.1016/j.indcrop.2010.02.010
6. Ioannidou O, Zabaniotou A (2007) Agricultural residues as precursors for activated carbon production—a review. Renew Sust Energ Rev 11:1966–2005. https://doi.org/10.1016/j.rser.2006.03.013
7. Rashidi NA, Yusup S (2017) A review on recent technological advancement in the activated carbon production from oil palm wastes. Chem Eng J 314:277–290. https://doi.org/10.1016/j.cej.2016.11.059
8. Nieto-Delgado C, Terrones M, Rangel-Mendez JR (2011) Development of highly microporous activated carbon from the alcoholic beverage industry organic by-products. Biomass Bioenergy 35:103–112. https://doi.org/10.1016/j.biombioe.2010.08.025
9. Nieto-Delgado C, Rangel-Mendez JR (2011) Production of activated carbon from organic by-products from the alcoholic beverage industry: surface area and hardness optimization by using the response surface methodology. Ind Crop Prod 34:1528–1537. https://doi.org/10.1016/j.indcrop.2011.05.014
10. Moreno-Piraján JC, Giraldo L (2012) Study of activated carbons by pyrolysis of Mangifera Indica seed (mango) in presence of sodium and potassium hydroxide. E-Journal Chem 9:780–785. https://doi.org/10.1155/2012/909747
11. Salas-Enrıquez BG, Torres-Huerta AM, Conde-Barajas E, Domınguez-Crespo MA, Dıaz-Garcia L, de la Negrete-Rodrıguez MLX (2016) Activated carbon production from the Guadua amplexifolia using a combination of physical and chemical activation. J Therm Anal Calorim 124:1383–1398. https://doi.org/10.1007/s10973-016-5238-8
12. Cobb A, Warms M, Maurer EP, Chiesa S (2012) Low-tech coconut shell activated charcoal production. Int J Serv Learn Eng 7:93–104
13. Suhas CPJM, Ribeiro Carrott MML (2007) Lignin-from natural adsorbent to activated carbon: a review. Bioresour Technol 98:2301–2312. https://doi.org/10.1016/j.biortech.2006.08.008
14. Adinata A, Wan Daud WMA, Aroua MK (2007) Preparation and characterization of activated carbon from palm shell by chemical activation with K_2CO_3. Bioresour Technol 98:145–149. https://doi.org/10.1016/j.biortech.2005.11.006
15. Gratuito MKB, Panyathanmaporn T, Chumnanklang RA, Sirinuntawittaya N, Dutta A (2008) Production of activated carbon from coconut shell: optimization using response surface methodology. Bioresour Technol 99:4887–4895. https://doi.org/10.1016/j.biortech.2007.09.042
16. Cruz DC (2012) Production of bio-coal and cctivated carbon from biomass. Dissertation, The University of Western Ontario. https://ir.lib.uwo.ca/cgi/viewcontent.cgi?article=2382&context=etd Accessed 30 June 2015
17. Etim UJ, Umoren SA, Eduok UM (2012) Coconut coir dust as a low cost adsorbent for the removal of cationic dye from aqueous solution. J Saudi Chem Soc 20:S67–S76. https://doi.org/10.1016/j.jscs.2012.09.014
18. Tan IAW, Ahmad AL, Hameed BH (2008) Preparation of activated carbon from coconut husk: optimization study on removal of 2,4,6-trichlorophenol using response surface methodology. J Hazard Mater 153:709–717. https://doi.org/10.1016/j.jhazmat.2007.09.014
19. Hoseinzadeh Hesas R, Arami-Niya A, Wan Daud WMA, Sahu JN (2013) Preparation of granular activated carbon from oil palm shell by microwave-induced chemical activation: optimisation using surface response methodology. Chem Eng Res Des 91:2447–2456. https://doi.org/10.1016/j.cherd.2013.06.004
20. Tsai WT, Chang CY, Lee SL (1998) A low cost adsorbent from agricultural waste corn cob by zinc chloride activation. Bioresour Technol 64:211–217. https://doi.org/10.1016/S0960-8524(97)00168-5
21. Yakub I, Mohammad M, Yaakob Z (2013) Effects of zinc chloride impregnation on the characteristics of activated carbon produced from physic nut seed hull. Adv Mater Res 626:751–755. https://doi.org/10.4028/www.scientific.net/AMR.626.751.
22. The National Institute for Occupational Safety and Health (NIOSH) (2018) Phosphoric acid. https://www.cdc.gov/niosh/npg/npgd0506.html. Accessed 25 November 2018.
23. The National Institute for Occupational Safety and Health (NIOSH) (2015) Zinc chloride. https://www.cdc.gov/niosh/ipcsneng/neng1064.html. Accessed 25 November 2018.
24. Anonymous (2010) Sodium chloride material safety data sheet. http://mpf.aap.cornell.edu/mpf/msds/printmaking/Intaglio/SodiumChloride.pdf. Accessed 26 November 2018.
25. Tang WK (1968) Effect of inorganic salts on pyrolysis of wood, cellulose, and lignin determined by differential thermal analysis. US For Serv Res Pap 82:1–37
26. Tooklang P, Vaivudh S, Sukchai S, Rakwichian W (2014) Thermal distribution performance of NPCM: NaCl, $NaNO_3$ and KNO_3 in the thermal storage system. Energy Power Eng 6:174–185
27. Mise S, Patil TN (2015) Adsorption studies of chromium(VI) on activated carbon derived from Mangifera indica (mango) seed shell. J Inst Eng Ser 96:237–247. https://doi.org/10.1007/s40030-015-0124-0
28. Calgon Carbon Coporation (2013) Product bulletin http://www.calgoncarbon.com/wp-content/uploads/product-literature/WPX.pdf. Accessed 6 July 2017
29. Montgomery DC (2012) Design and analysis of experiments. Wiley & Sons Inc, New York
30. ASTM International (1999), Standard test methods for moisture in activated carbon. ASTM Standard D2867. https://doi.org/10.1520/D2867-09.2
31. ASTM International (2004) Standard test method for total ash content of activated carbon. ASTM Standard D2866. https://doi.org/10.1520/D2866-11.2

32. ASTM International (2004) Standard test method for volatile matter content of activated carbon samples. ASTM Standard D 3175. https://doi.org/10.1520/D5832-98R08.2
33. Sluiter A, Hames B, Ruiz RO, Scarlata C, Sluiter J, Templeton D et al (2008) Determination of structural carbohydrates and lignin in biomass. htpps://doi.org/NREL/TP-510-42618
34. Molina-Sabio M, RodRíguez-Reinoso F, Caturla F, Sellés MJ (1995) Porosity in granular carbons activated with phosphoric acid. Carbon 33:1105–1113. https://doi.org/10.1016/0008-6223(95)00059-M
35. Mianowski A, Owczarek M, Marecka A (2007) Surface area of activated carbon determined by the iodine adsorption number. https://doi.org/10.1080/00908310500430901
36. AlOthman Z, Habila M, Ali R (2011) Preparation of activated carbon using the copyrolysis of agricultural and municipal solid wastes at a low carbonization temperature in: 2011 Int Conf Biol Environ Chem Singapore, pp. 67–72. http://www.ipcbee.com/vol24/14-ICBEC2011-C00040.pdf. Accessed 30 June 2015
37. Setoyama N, Kaneko K, Rodriguez-Reinoso F (1996) Ultramicropore characterization of microporous carbons by low-temperature helium adsorption. J Phys Chem 100:10331–10336. https://doi.org/10.1021/jp960467p
38. Linares-Solano A, Salinas-Maritnez C, Alcafiiz-Monge J, Cazorla-Amoros D (1988) Further microporous advances carbons in the characterization by physical adsorption of of gases. Tanso 185 (1998) 316–325. https://doi.org/10.7209/tanso.1998.316
39. Lozano-Castello D, Cazorla-Amoros D, Linares-Solano A (2004) Usefulness of CO_2 adsorption at 273 K for the characterization of porous carbons. Carbon 42:1231–1236. https://doi.org/10.1016/j.carbon.2004.01.037
40. de Jonge H, Mittelmeijer-Hazeleger MC (1996) Adsorption of CO_2 and N_2 on soil organic matter: nature of porosity, surface area, and diffusion mechanisms. Environ Sci Technol 30:408–413. https://doi.org/10.1021/es962011r
41. Gergova K, Petrov N, Eser S (1994) Adsorption properties and microstructure of activated carbons produced from agricultural by-products by steam pyrolysis. Carbon 32:693–702. https://doi.org/10.1016/0008-6223(94)90091-4
42. Elizalde-González MP, Hernández-Montoya V (2007) Characterization of mango pit as raw material in the preparation of activated carbon for wastewater treatment. Biochem Eng J 36: 230–238. https://doi.org/10.1016/j.bej.2007.02.025
43. Ola FA, S.O. Jekayinfa SO (2014) Ref: C0605 pyrolysis of mango stone shell: effect of heating temperature and residence time on product yields. Pages 1–8. http://www.geyseco.es/geystiona/adjs/comunicaciones/304/P06050002.pdf. Accessed 4 June 2015
44. Yang H, Yan R, Chen H, Lee DH, Zheng C (2007) Characteristics of hemicellulose, cellulose and lignin pyrolysis. Fuel 86:1781–1788. https://doi.org/10.1016/j.fuel.2006.12.013
45. Silgado KJ, Marrugo GD, Puello J (2014) Adsorption of chromium (VI) by activated carbon produced from oil palm endocarp. Chem Eng Trans 37:721–726. https://doi.org/10.3303/CET1437121
46. Qiao Z, Wang Y, Gao Y, Li H, Dai T, Y. Liu Y (2010) Commercial activated carbons as the sources for producing multicolor photoluminescent carbon dots by chemical oxidation. Chem Commun 46: 8812–8814. https://doi.org/10.1039/C0CC02724C
47. Campbell QP, Bunt JR, Kasaini H, Kruger DJ (2012) The preparation of activated carbon from South African coal. J South African Inst Min Metall 112:37–44
48. Pakuła M, Walczyk M, Biniak S, Światkowski A (2007) Electrochemical and FTIR studies of the mutual influence of lead(II) or iron(III) and phenol on their adsorption from aqueous acid solution by modified activated carbons. Chemosphere 69: 209–219. https://doi.org/10.1016/j.chemosphere.2007.04.028
49. Peng H, Wang N, Hu Z, Yu Z, Liu Y, Zhang J, Ruan R (2012) Physicochemical characterization of hemicelluloses from bamboo (Phyllostachys pubescens Mazel) stem. Ind Crop Prod 37:41–50. https://doi.org/10.1016/j.indcrop.2011.11.031
50. Henrique MA, Silverio HA, Flauzino Neto WP, Pasquini D (2013) Valorization of an agro-industrial waste, mango seed, by the extraction and characterization of its cellulose nanocrystals. J Environ Manag 121:202–209. https://doi.org/10.1016/j.jenvman.2013.02.054